Vehicle-Scale Investigation of a Fluorine-Hydrogen Main Tank Injection Pressurization System

E. C. CADY* AND D. W. KENDLE†
McDonnell Douglas Astronautics Company
Huntington Beach, Calif.

A comprehensive analytical and experimental program that resulted in an advanced computerized analysis for predicting the performance of a fluorine-hydrogen Main Tank Injection (MTI) pressurization system for LH_2-fueled space vehicles is described. Accuracy of the analysis was verified by a series of 17 tests of a full-scale MTI pressure control system in a 1000 ft^3 flight-weight LH_2 tank. Prepressurization, constant- pressure hold, and LH_2 expulsion at controlled tank pressure were demonstrated over a wide range of ullage volumes, pressures, flowrates, and injector configurations, with reasonable ullage gas and tank-wall temperature and efficient fluorine usage.

Nomenclature

a = acceleration
C = constant
d = jet exit diameter
f = injector on-time fraction
f_m = ullage mixing fraction
$\dot{q}$ = heat-transfer rate
T = temperature
U = velocity
W = molecular weight
X = distance on the vertical axis
Δ = increment
ρ = density

Subscripts

b = buoyancy
C = jet velocity core
F, F_2 = flame, fluorine
g = gas
H_2, HF = hydrogen, hydrogen fluoride
J = injectant jet flow
L = liquid
m = maximum
M = turbulent mixing
mix = ullage mixing
P = jet penetration
r = reaction
u = ullage
o = initial

I. Introduction

FOR cryogenic vehicles, particularly those that require multiburn operation, the tank pressurization system can contribute significantly to the weight, complexity, and cost of the propulsion feed system. A tank pressurization concept termed main tank injection (MTI) is a means to reduce weight and increase system simplicity. In this concept, a hypergolic reactant is injected into a propellant tank and the resultant heat release pressurizes the tank. When controllable, this technique promises considerable performance and cost improvement, especially for an advanced hydrogen-fueled upper stage.

A previous program[1] conducted under NASA Contract NAS 3-7963 determined the feasibility, limitations, and operating characteristics of a small-scale, fluorine-hydrogen MTI pressurization system; also, it indicated the need for an analytical method to predict MTI performance for any size of LH_2-fueled space vehicle, and for the development and demonstration of a full-scale, flight-type MTI pressurization system. This paper describes a comprehensive program to determine analytically and experimentally the applicability of fluorine-hydrogen MTI to LH_2-fueled space vehicles. The program approach was as follows: 1) a computerized analytical technique was developed to predict the performance of a flight-type MTI pressure control system, 2) a large-scale MTI control system was designed and fabricated, and 3) 17 tests were performed in a 1000 ft^3 flight-weight LH_2 tank. The analysis was correlated to the test results and used to predict the performance of an MTI pressure control system for a Centaur vehicle configuration and mission specified by NASA.

II. Analytical Study

The tank, propellant, and ullage are represented by a one-dimensional model. Variations in temperatures and temperature-dependent properties occur only along the vertical tank axis with no radial or circumferential variations. This model is the basis for several analyses of conventional heated-gas tank pressurization[2-3] and its validity is well established. Buoyant forces caused by gravity or vehicle acceleration tend to produce a stable thermal stratification in the gas and liquid, resulting in a temperature distribution that is essentially one-dimensional.

The computations are based on a finite-difference representation of the physical system. The tank wall, internal hardware, propellant, and ullage are each divided by horizontal planes into a number of nodes as shown schematically in Fig. 1, with the properties within each node being uniform. The axial thickness and location of the gas and liquid nodes can vary during the solution, while the wall and hardware nodes are of equal thickness and fixed.

Ullage mixing is a key feature of the MTI analysis. The injectant inflow causes gas mixing in the region near the injector, resulting in a nearly-uniform temperature in the top part of the ullage. This mixed zone is represented by the large, single, upper gas node shown in Fig. 1. Nonuniformities exist directly in the injectant flow path, particularly with the MTI flame; however, in the vicinity of the wall heat-transfer surface, a nearly-uniform temperature is maintained in the mixing zone.

The extent of the mixed ullage region is directly related to the depth of penetration into the ullage of the downward-flowing injectant jet. The velocity of this jet decreases with

Presented as Paper 71-645 at the AIAA/SAE 7th Propulsion Joint Specialist Conference, Salt Lake City, Utah, June 14–18, 1971; submitted June 24, 1971; revision received September 27, 1971. This work was sponsored by NASA-Lewis Research Center under Contract NAS 3-13306.

*Senior Engineer. Member AIAA.
†Senior Engineer/Sciences. Associate Member AIAA.

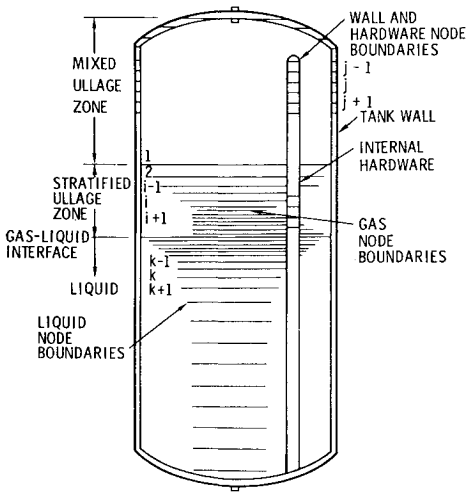

Fig. 1 Finite difference node system.

distance from its origin due to buoyancy because it is at higher temperature and lower density than the ullage and because of viscous mixing with the surroundings. These processes slow the jet to a zero axial velocity at some point, which is the jet penetration limit. An analysis for predicting this jet penetration depth was developed initially for nonreacting jets[5] and was extended to the reacting MTI case.

The basic equation for the deceleration of the jet centerline velocity because of buoyancy is

$$1/2\rho_j d(U_j^2) = a(\rho_j - \rho_u)dX \tag{1}$$

or

$$\mathrm{d}(U_j^2) = 2\mathrm{a}[1 - (\rho_u/\rho_j)]dX \tag{2}$$

Because the ullage may be near LH_2 temperatures initially, a compressibility factor is included in the equation for ρ_u but the warmer jet is assumed to be a perfect gas; Eq. (2) becomes

$$\mathrm{d}(U_j^2) = 2a[1 - (T_j/W_j)(W_u/Z_uT_u)]dX \tag{3}$$

where T_j is the temperature and W_j is the molecular weight on the centerline of the jet, which vary with distance X in the flame structure. The variation in velocity because of turbulent jet mixing must also be specified.

For the nonreacting jet analysis,[5] the equations of Laufer[6] were used for T_j, W_j, and the velocity decay caused by jet mixing. The same equation form is used for the reacting jet. The centerline velocity variation caused by viscous mixing only is assumed to be unaffected by the MTI reaction

$$U_j/U_{jo} = X_c/X \qquad X > X_c \tag{4}$$

where X_c is the velocity core length. The temperature equation is modified by using the flame length X_F as the effective temperature core length

$$(T_j - T_o)/(T_{jm} - T_o) = X_F/X \qquad X > X_F \tag{5}$$

In the flame region, a linear increase in centerline temperature is assumed

$$(T_j - T_{jo})/(T_{jm} - T_{jo}) = [(X - X_c)/(X_F - X_c)]X_c < X \leq X_F \tag{6}$$

and T_j remains equal to T_{jo} in the velocity core region ($X < X_c$). The centerline gas composition is also given by Eqs. (5) and (6), replacing the left side of both by Y_j, the mass fraction of HF which is equal to one at the maximum temperature point and zero in the surrounding medium, and at the jet exit. The jet centerline molecular weight is then given by

$$W_j = W_oW_{HF}/[Y_j(W_o - W_{HF}) + W_{HF}] \tag{7}$$

where $W_o = W_{H2}$ for $X > X_F$ and $W_o = W_{F2}$ for $X_c < X \leq X_F$.

The values of X_c and X_F were determined empirically. The velocity core length was evaluated[5] from nonreacting jet test data

$$X_c = 23.0[\rho_{jo}d^2/8\rho_u]^{1/2} \tag{8}$$

The flame length was measured from photographic data taken during the NAS 3-7963 tests[1] and defined as

$$X_F = X_c + 67d \tag{9}$$

where both X_c and X_F are measured from the jet exit.

The centerline velocity-squared decrement caused by buoyancy forces on the hot, downward flowing jet is found by combining and intergrating the above equations, giving three different equations for the three regions of the jet structure: the velocity core, the flame zone, and beyond the flame zone. Velocity core zone ($X \leq X_C$)

$$\Delta(U_j^2)_a\Big|_{x_1}^{x_2} = 2s\left(1 - \frac{T_{jo}W_{H2}}{W_{F2}Z_uT_u}\right)(X_2 - X_1) \tag{10}$$

Flame zone ($X_c < X \leq X_F$)

$$\Delta(U_j^2)_b\Big|_{x_1}^{x_2} = 2a\left\{A(X_2 - X_1) + \frac{B}{2}\left[(X_2 - X_c)^2 - (X_1 - X_c)^2\right] + \frac{C}{3}\left[(X_2 - X_c)^3 - (X_1 - X_c)^3\right]\right\} \tag{11}$$

$$A = 1 - (T_{jo}W_{H2}/W_{F2}Z_uT_u)$$

$$B = -\frac{W_{H2}[T_{jo}(W_{F2} - W_{HF}) + W_{HF}(T_{jm} - T_{jo})]}{W_{F2}W_{HF}Z_uT_u(X_F - X_c)}$$

$$C = -\frac{W_{H2}(W_{F2} - W_{HF})(T_{jm} - T_{jo})}{W_{F2}W_{HF}Z_uT_u(X_F - X_c)^2}$$

Beyond the flame zone ($X > X_F$):

$$\Delta(U_j^2)_b\Big|_{x_1}^{x_2} = 2a\left[D(X_2 - X_1) + E\ln\left(\frac{X_2}{X_1}\right) - F\left(\frac{1}{X_2} - \frac{1}{X_1}\right)\right] \tag{12}$$

$$D = 1 - (T_o/Z_uT_u)$$

$$E = -\frac{X_F[T_o(W_{H2} - W_{HF}) + W_{HF}(T_{jm} - T_o)]}{W_{HF}Z_uT_u}$$

$$F = -\frac{X_F^2(W_{H2} - W_{HF})(T_{jm} - T_o)}{W_{HF}Z_uT_u}$$

In all regions of the jet flow, the centerline velocity-squared decrement from location X_1 to X_2 caused by turbulent mixing with the surrounding ullage is given by

$$\Delta(U_j^2)_M\Big|_{x_1}^{x_2} = U_{jo}^2X_c^2\left(\frac{1}{X_2^2} - \frac{1}{X_1^2}\right) \tag{13}$$

from Eq. (4). The total centerline velocity-squared decrement is the sum of the mixing and buoyancy contributions

$$\Delta(U_j^2)\Big|_{x_1}^{x_2} = \Delta(U_j^2)_M\Big|_{x_1}^{x_2} + \Delta(U_j^2)_b\Big|_{x_1}^{x_2} \tag{14}$$

where the mixing contribution is zero when $X < X_c$.

Equation (14) determines the jet penetration depth X_p at which the centerline velocity has decreased to zero. The depth of the mixed ullage zone X_{mix} may be less than X_p, therefore

$$X_{\mathrm{mix}} = f_mX_p \tag{15}$$

defines a mixing fraction factor f_m, which is a measure of the effectiveness of the ullage mixing.

The jet penetration and ullage partial mixing models are of

primary importance to the over-all MTI pressurization analysis. All heat released by the flame goes into the mixed zone because this is the region directly affected by the injectant flow. Forced convection heat transfer to the tank wall occurs in this region, which is agitated by the gas mixing. The heat and mass transfer at the gas-liquid interface are determined by the injectant jet penetration because the dominant mode of interface heat transfer results from direct impingement of the injectant flow upon the liquid surface. Other aspects of the analysis are similar to that of a conventional heated-gas pressurization system.

The MTI pressurization computer program[7] incorporating the aforementioned features includes essentially all capabilities of existing pressurization programs: variable properties for the gas, liquid, wall, and internal hardware; unrestricted tank configuration; injectant supply system computations; operating parameters specified by either time-variable tabular inputs or internal calculations; and a number of different operating modes. In normal usage, the fluorine supply system and propellant outflow rates are specified and the computer program calculates the temperature distributions in the wall, hardware, liquid, and gas, as well as the liquid vaporization rate and tank pressure, all of which vary with time during the solution. These data may be output from the program as frequently as desired.

III. Experimental Investigation

The experimental investigation for this program had two principal objectives: 1) to provide experimental data to verify the analytical model, to evaluate empirical parameters in the analysis, and to establish the accuracy of MTI system performance predicted by the computer program, and 2) to design, fabricate, and successfully demonstrate an MTI control system and injectors in a large-scale, flightweight LH_2 test tank. The design requirements for the MTI control system were: 1) self-regulating, 2) capable of controlled pressurization, pressure hold, and expulsion at varied outflow rates up to a maximum of 15 lb/sec of LH_2, 3) operable at any ullage volume, 4) capable of a wide range of flowrates and operating pressures, 5) able to pressurize the tank to within 1 psi of the desired pressure, 6) capable of safe operation without damage to the injector or tank, freezing of fluorine in the injector, and causing minimum heat leakage into the tank when not in operation.

A control system was designed to sense tank pressure and open and close the GF_2 injector valve to maintain the tank pressure within a narrow band (so-called "bang-bang" system). Important elements are the pressure switch, the injector valve, and the injector. The pressure switch system used completely-redundant, invidually-plumbed, mercury-type pressure switches (Mercoid type APH-41-153) with a range of 15 to 45 psia and a maximum actuation band of ± 0.375 psi. This switch would not be suitable for flight vehicle use because the mercury element must be level and is thus g-vector sensitive. Bellows-type switches suitable for flight use with the same fast response and narrow actuation band are available, but were too expensive for this program. The injector valve was a modified Fox Valve Development Co. type 610851 valve used successfully on the previous MTI program. This valve has a copper-on-stainless steel seat and is compatible with liquid and gaseous fluorine. The valve was actuated by 500-psia helium through two integral solenoids, one to actuate open and the other to actuate closed. The high-pressure helium actuation enabled extremely fast valve response (closed to full-open or vice versa in less thatn 10 msec).

The straight-pipe injector is the best design for MTI pressurization for the following reasons. 1) The heat of reaction from the injectant must be distributed to a large mass of gas to prevent excessive local temperatures in the ullage. NASA experimental data[8] and MDAC analysis[5] indicate that the straight-pipe injector gives the greatest ullage penetration and mixing, and, subsequently, the highest pressurization performance. 2) The straight-pipe injector was successfully tested in the previous MTI Contract NAS 3-7963 where it performed efficiently and reliably in the MTI pressurization environment. 3) The straight-pipe injector is simple and easy to fabricate. A comprehensive analysis of injector performance indicated that a 1-in.-diam straight-pipe would give reasonable inlet velocities (of the order of 20–100 fps), adequate ullage mixing, and sufficient LH_2 vaporization to assure reasonable ullage temperatures.

The injector would normally be located on the tank centerline, but the only available port into the Thor test tank was offset. The straight-pipe injector thus had to be fairly long (~ 35 in.) to reach to the tank centerline. An offset injector location was also used to investigate the influence of injector-to-wall distance on the gas-wall heat transfer coefficients.

The downward penetration of the injectant from the straight-pipe injector varies inversely with the local acceleration (or g-level). The penetration of a straight-pipe injector may be acceptable in one-g, but may be excessive under low-g prepressurization conditions. Impingement on the liquid surface could cause sloshing and bubble entrapment which could be deleterious to vehicle operation. Reduced penetration for low-g prepressurization can be achieved with a diffuser-type injector. Analysis resulted in a conical diffuser design that divided the inflow into a number of small gas streams. Each gas jet penetrates and mixes with the ullage in the same general manner as the straight-tube inflow, but the depth of penetration is greatly reduced because of the smaller size of the individual gas streams.

The baseline diffuser was designed with a total flow area equal to the 1-in.-diam straight-pipe so that equal initial flow velocities at the injector were realized with equal GF_2 flowrates. This reduced the number of parametric differences between the two injector types. The cone half-angle was set at 15° to assure adequate spreading without danger of the flame impinging on the tank wall. The analysis further indicated that for propellant settling accelerations typical of a space vehicle (e.g., 10^{-3}–$10^{-2}g$) a 25-hole 15° diffuser would have a penetration distance nearly identical to the straight-pipe at normal gravity. The pressurization performance for this diffuser in low-g should be similar to the one-g straight-pipe test data.

During the test program under Contract NAS 3-7963, injectors fabricated from copper were found to provide maximum resistance to burning because of their high thermal conductivity that tends to eliminate hot spots and injector ignition with the fluorine; therefore, both injectors were fabricated from oxygen-free copper.

Preliminary testing of the fluorine injection system was performed by hot-firing the injectors in a cold GH_2 atmosphere with GF_2 flow on-off cycle rates simulating the injector cycling anticipated in the Thor tank tests. The purpose of these tests was fourfold, 1) to verify the structural adequacy of the injectors and reveal any injector burning problems which could occur, 2) to determine that injectant (GF_2) freezing would not occur in the long injector tube, 3) to verify the proper operation of the MTI control system, 4) to verify the proper operation of the GF_2 supply system and evaluate the accuracy of the GF_2 flowrate measurement technique.

The straight-pipe and showerhead-diffuser injector designs performed properly with no evidence of injector burning or injectant freezing. An alternate diffuser design was destroyed during these tests and was dropped from further consideration. The MTI control system and GF_2 supply system performed nominally. The GF_2 flowrate measurement technique was modified to improve accuracy during the pressurization tests in the test tank.

The flight-weight test tank was a Thor missile oxidizer

tank made of 2014-T6 aluminum, internal waffle-pattern milled to a minimum wall thickness of 0.050 in. The tank had a 95.5-in. inside diameter, a 228-in-long cylindrical section, and 16.8-in.-high spherical segment end domes. An insulation system of closed-cell polyurethane foam (Perma-foam type CPR385D) with a density of 2 lb/ft^3 and a thermal conductivity of 0.16 Btu/hr-°R-ft^2/in. was installed. Assuming an external foam temperature of 30°F, $2\frac{1}{2}$ in. of this foam was calculated to limit the heat flux into the Thor tank to about 30 Btu/hr-ft^2.

The test tank was installed at the Alpha Complex, Test Stand 1 at the MDAC Sacramento Test Center. The complex has an LH_2 capacity of 90,000 gallons and extensive supplies of N_2 and He purge gases. The GF_2 supply system used in the injector hot-firing tests was installed at the test stand and plumbed to the injector assembly in the test tank dome. The test tank had provisions for venting, purging, LH_2 fill, variable LH_2 outflow, LH_2 sampling for HF contamination, plus tank pressurization with both He and GH_2.

Over 100 channels of data were acquired during the test program. Gas, liquid, and wall temperatures were measured with platinum resistance thermometers. Tank pressure (redundant) and the upstream pressure and ΔP across the GF_2 flow-measuring orifice were measured with strain-gage transducers. The internal tank instrumentation is shown in Fig. 2. The sensors to measure ullage gas and liquid temperature were mounted at 1-ft intervals on a vertical probe at the half-radius of the tank.

Every third sensor was set to measure LH_2 temperature, which coincided with the location of the level sensors. At the basic fill levels of 95, 50, and 10%, the LH_2 temperature sensors also provided the reference temperature for seven-element thermopile assemblies used to determine the initial conditions at the interface. The thermopiles measured the temperature differences between junction levels 1 in. apart vertically. Carbon resistor level sensors were mounted in pairs 1 in. apart on the vertical probe at the three liquid fill levels (95+, 95, 50+, 50, 10+ and 10%). The initial liquid level was kept between these 1-in.-apart sensors. These level sensors plus single units at 80, 65, 35, and 20% liquid levels were used for LH_2 outflow rate measurement. The tank wall temperatures were measured at eight locations where sensors were bonded to the outside of the tank wall under the foam insulation.

The heat flux to the tank wall was measured at 11 locations with polyimide glass-thermopile fluxmeters. The ullage gas temperature near the flux-meters was also measured. The fluxmeters were mounted on the vertical channels as shown in Fig. 2.

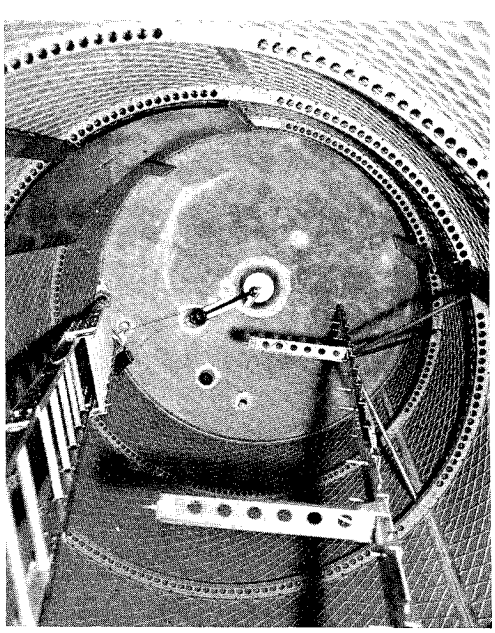

Fig. 2 Internal view of test tank instrumentation.

The test plan included a matrix of test runs allowing examination of the effects of a number of variables on the MTI pressurization process: injector configuration, initial ullage volume and condition, GF_2 injection flowrate and velocity, LH_2 outflow rate, tank pressure, and test cycle (prepressurization, hold, and expulsion). Three GF_2 injector configurations were tested: 1) the straight-pipe centerline, 2) the straight-pipe offset, and 3) the diffuser centerline. The straight-pipe injector located on the tank centerline is the conventional configuration for an MTI pressurization system and was used with the most extensive range of test conditions. The straight-pipe injector at the offset location provided a variation in the injector-wall distance to evaluate the effect on gas-wall heat-transfer rates. The diffuser injector decreases the penetration of the GF_2 injectant into the GH_2 ullage; its behavior was of general interest in the verification of the MTI model and to demonstrate this injector design for low-g prepressurization applications. The major test parameters were the ullage volume (90, 50, and 5%), and the GF_2 injector inlet velocity (controlled by the GF_2 bottle pressure). Two basic tank pressures of 43 psia and 24 psia were used and two LH_2 outflow rates (5 and 15 lb/sec). However, 15 lb/sec could not be achieved with 24-psia tank pressure.

Detailed results of the test program are described in Ref. 7. The reponse of the MTI Control System is shown in Fig. 3 for a 5% ullage test (the most severe in terms of pressure response). The two traces shown are for the two fully-redundant pressure transducers. The pressure rises rapidly from 15.6 psia to 44.4 psia, then cycles quite slowly during the hold period, with the valve open only about 4% of the time. The maximum pressure band at this time is 3.0 psi. Fig. 4 indicates the change that occurs in the pressure cycle

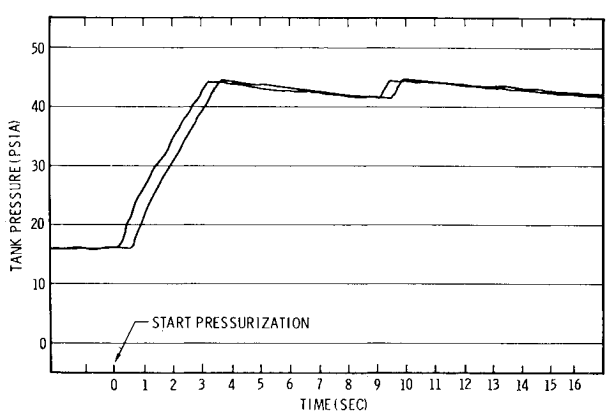

Fig. 3 Control system response—5% ullage—prepressurization.

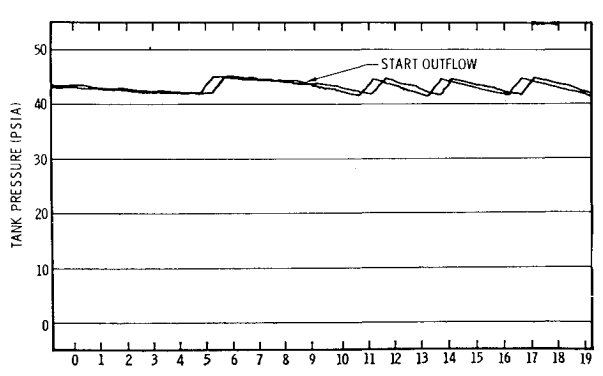

Fig. 4 Control system response—5% ullage—outflow.

when LH_2 outflow starts. The cycle rate increases with the injector on about 18% of the time. As the test progresses, the injector-on fraction gets larger (toward the end of the test, the valve may be open all of the time) and the control band gets narrower. The response of the control system with 50 and 90% initial ullage is similar, except that prepressurization is slower and the control band is narrower (1.2 psi with 90% ullage). The data indicated that the control system was capable of controlling tank pressure at any ullage volume with prepressurization, hold and expulsion cycles, and at varied LH_2 outflow rates.

IV. Analysis of Experimental Results

Two important quantities predicted by the MTI computer program are the GF_2 usage and the ullage temperature. These values are strongly influenced by three major components of the MTI analysis: 1) ullage mixing, 2) heat transfer to the liquid and propellant vaporization, and 3) gas-wall heat transfer. The models for these processes include empirical parameters that must be evaluated through correlation with the experimental data.

The ullage mixing model assumes a uniform gas temperature in the mixed zone. Evaluation of the temperature profile data from the experimental program indicates this assumption is a good approximation although it is not strictly true in many cases. Some variations in gas temperature do occur in the mixed region and the degree of stratification tends to increase with time during a pressurization test. However, the net effect on pressurization performance is adequately described by the model. The mixed ullage temperature is an average value for the actual temperature distribution in this region and gives the proper gas-wall heat transfer. The total mass of gas involved in injectant reaction heating is accurately defined by the mixing depth because the calculated rate of temperature increase agrees with the experimental behavior.

The jet penetration depth X_P was not directly measured in the tests. However, two observations from the data correlations indicate the general accuracy of this calculation: the ullage mixing depth X_{mix} did not exceed and was in some cases equal to X_P, so that the calculated X_P was a limiting value for the observed X_{mix}, as assumed; and propellant vaporization, caused by jet impingement on the liquid surface and determined by ullage mass balance, was observed to cease at the time when the calculated X_P became less than the ullage depth. These observations indicated no need for modification of the jet penetration analysis. In relating the ullage mixing depth to the jet penetration, the model compensates for nonideal behavior of the physical system through use of the ullage mixing fraction factor f_m defined in Eq. (15).

The injectant jet velocity provides the energy for the ullage mixing process. Ideally, this energy would be dissipated in random turbulent motion throughout the ullage volume to the full depth of the jet penetration and would maintain uniform conditions in this region. The experimental data suggest the existence of a circulating flowfield in the mixed zone rather than purely random motion. The net result is a mixing depth less than the penetration depth and some degree of thermal stratification, giving a mixing fraction factor $f_m < 1$.

Correlating computer program predictions with the data from tests with 50 and 90% initial ullages (no liquid evaporation) determined that $f_m = 0.8$ gave good agreement with both the ullage temperature profiles and the GF_2 usage. Figure 5 shows the calculated mixed-ullage temperatures (the heavy, vertical line segments) compared to experimental data for one of the tests. The calculated stratified temperature profile below the mixed zone is not shown. This value of f_m was then used in the correlations with the 5% initial ullage tests to determine the interface heat-transfer parameters.

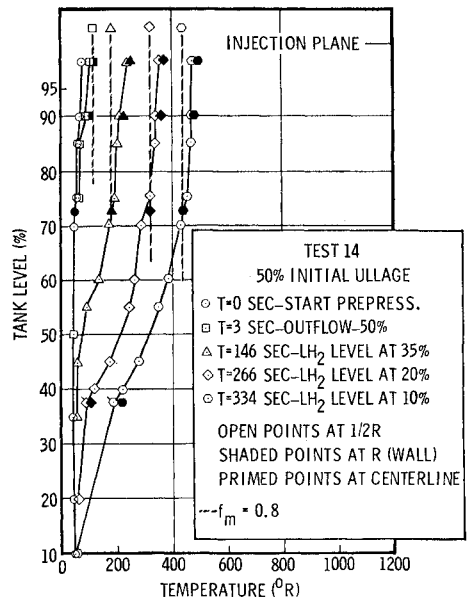

Fig. 5 Temperature correlation for test 14.

The heat-transfer rate from the ullage gas to the liquid interface is described by

$$\dot{q}_g = CX_L^2 \tag{16}$$

where X_L, the depth of penetration into the LH_2 by the injectant jet, is calculated in the same general manner as the ullage penetration depth X_P. This parameter was chosen to control the calculated heat-transfer rate because the area exposed to the impinging flow, the degree of disturbance to the surface, and the gas velocity near the surface all increase with increasing X_L. The second power dependence on X_L was tentatively established from correlations with LH_2 tank pressurization data[8] and was confirmed by the MTI test data. Because heat transfer occurs directly from the impinging injectant jet, the coefficient C is related to the heat available in this jet $\dot{q}_r$ which is released from the F_2/H_2 reaction; $C = 0.6\ \dot{q}_r$ was determined from the correlation. Heat losses to raising the liquid temperature $\dot{q}_L$ were 20% of $\dot{q}_g$ while 80% went to vaporization. The LH_2 evaporation predicted by these empirical relationships agreed well with the addition rates calculated from the experimental ullage mass balance data.

The low-pressure, small-ullage tests were exceptions to the generally good correlations obtained with the aforementioned empirical factors. A much better fit was obtained with $f_m = 0.9$ and with the interface transfer independent of X_L, $\dot{q}_g = 0.25\ \dot{q}_r$. Essentially all heat transferred to the interface went to liquid vaporization with $\dot{q}_L = 0$. A comparison of calculated and experimental temperature distributions for test 7 is shown in Fig. 6. One characteristic of these tests that could explain this different behavior is the very short injector valve on-time (<0.5 sec). A short flow time may not permit the injectant jet to establish the same steady-state flowfield in the ullage obtained in the other tests, resulting in different performance response. An attempt to include the injector on-time as a parameter in the empirical equations or to define a criterion for selecting between the two sets of empirical factors was not successful. The available data did not permit such a complex correlation.

The multiple-jet spreading flow from the diffuser-injector presents an ullage flowfield significantly different from that of the straight-pipe injector. More-extensive interaction with the ullage and more-effective gas mixing by this spreading flow results in $f_m = 1.0$ for this configuration. Figure 7 shows the good temperature profile correlation obtained

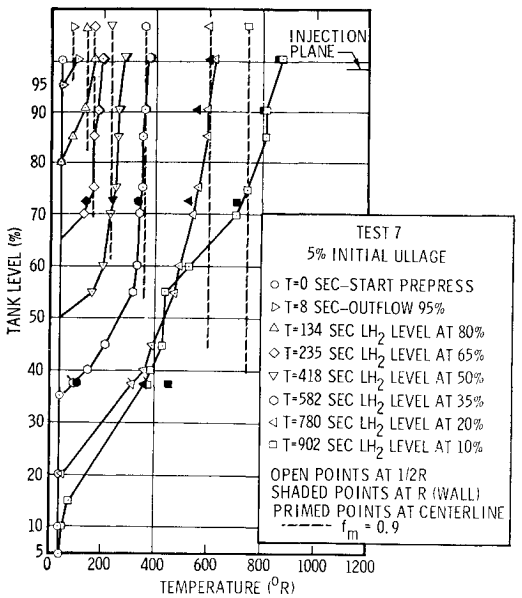

Fig. 6 Temperature correlation for test 7.

with this value, indicating that ullage mixing extends to the full depth of injectant jet penetration for diffuser injectors.

Heat-transfer data taken at the tank wall locations in the mixed ullage region indicated heat-transfer rates in excess of that accounted for by free convection. This excess was assumed to be the forced convection contribution. Using an established equation for forced convection to a vertical flat plate,[9] the gas velocity was determined which gave the experimental coefficient value. This velocity at the wall was related to the GF_2 velocity at the injector tip and to the injector on-time fraction by

$$U = 0.12U_{jo}f \tag{17}$$

This relationship was used in all of the performance calculations.

Comparison of the predicted and actual GF_2 usage is shown in Table 1 for the first four tests (which include 5, 50, and 90% initial ullage cases). Using the appropriate correlation values generally gave GF_2 usage prediction for all tests within $\pm 15\%$.

An ullage mass balance and ullage gas and tank-wall enthalpy balance was computed for each test. When conditions in the ullage changed slowly, the temperature sensors were able to respond adequately and the mass balance gave reasonable results. With large-ullage pressurization, sensor lag led to initial errors in the mass balances; however, when conditions settled down to less-rapid change, the computed mass generally returned to within 10% of original values. The results confirmed the assumption that LH_2 evaporation and ullage mass addition did not occur with large ullages.

Table 1 Comparison of predicted and actual GF_2 usage

Test	Time sec	Actual GF_2 weight, lb	Predicted GF_2 weight, lb	Error, %
1	12.7	0.912	0.955	+5.1
2	19.2	1.290	1.102	−14.6
	85	1.730	1.480	−14.5
	144	3.630	3.127	−13.9
	196	5.630	5.380	−4.5
	230	6.680	6.800	+1.8
3	59	3.52	3.78	+7.4
	133	5.42	5.44	+0.4
4	4	0.190	0.196	+3.2
	23	0.416	0.196	...
	65	1.200	0.976	−18.6
	109	2.610	2.480	−5.0

The mass balances for the small-ullage cases give better results because of slower changes in temperature. These are shown in Table 2 and compared with the predicted evaporation. Test 7 has slowly changing, well-mixed ullage conditions and gives excellent mass computations; evaporation occurs up to a time of 235 sec (when the computed liquid penetration stops), and is constant after that time. At a time of 902 sec, the computed mass jumped over 2 lb because of the unexplained temperature reversal anomaly at the 55% level (see Fig. 7).

The enthalpy balances were also rather imprecise because of temperature sensor lag. Figure 8 shows a typical result with the distribution of injected energy to ullage, tank, and liquid. Inaccuracy in the measured wall temperature distributions is probably the principle source of error.

Figures 5–7 show that the average ullage gas temperature near the tank wall (the shaded points) was very close to the temperatures recorded at the half-radius probe, which substantiates the assumption of radial ullage uniformity.

Further, Test 7 with the centerline injector (Fig. 6) and Test 14 with the offset injector (Fig. 5) show no significant radial temperature distribution, indicating good radial

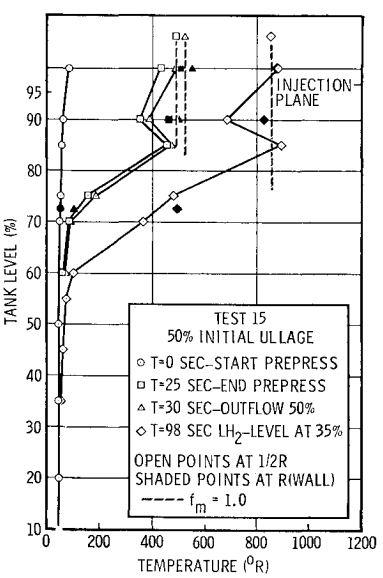

Fig. 7 Temperature correlation for test 15.

Table 2 Mass Balances—5% ullage

Test	Time, sec	Ullage mass computed from temperature data, lb	Predicted ullage mass, lb
4	0	5.919	5.919
	23	6.483	7.935
	65	10.649	9.830
	109	10.309	9.929
5	0	5.652	5.652
	75	7.415	10.340
	130	11.995	12.649
	164	14.688	12.840
	215	11.098	12.962
7	0	6.073	6.073
	8	6.216	6.159
	134	10.435	8.926
	235	12.097	12.355
	418	12.202	12.817
	582	12.455	12.934
	780	12.209	13.055
	902	15.044	13.090

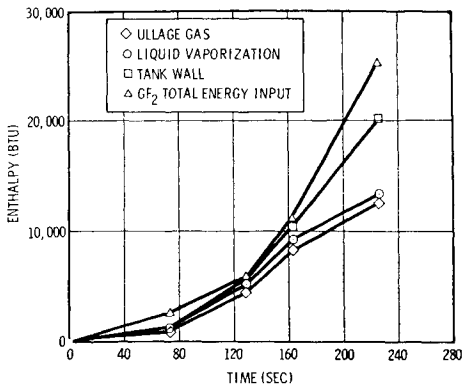

Fig. 8 Energy distribution—5% ullage—test 5.

mixing regardless of injector location. The greatest difference is with the diffuser injector at the 90% level which was attributed to a local gas circulation pattern caused by the diffuser spread angle.

To demonstrate the applicability of the MTI analysis to large-scale flight vehicles, a vehicle configuration and mission specified by NASA was analyzed to determine the performance of an MTI pressurization system. The Centaur vehicle was specified with a total LH_2 tank volume of 1240 ft^3 and a 0.016-in.-thick 316 stainless steel tank wall. The mission requirements were to provide three prepressurization cycles (at ullage volumes of 65, 380, and 1000 ft^3) plus hold periods with low outflow for engine chilldown. The expulsion pressurization requirements were to be provided by high-pressure GH_2 bled from the engines so that MTI was not used for expulsion.

A straightforward MTI pressurization system was designed with ambient GF_2 storage in a 400-psia aluminum sphere, an injector valve, and a diffuser injector (because of 10^{-3} g_e settling thrust during prepressurization). The analysis indicated GF_2 requirements of 0.058, 0.256, and 0.549 lb for the three pressurizations for a total of 0.863 lb. It was assumed that 3 lb of GF_2 were stored with a total system weight of 16.7 lb. The LH_2 evaporated during the first prepressurization was calculated to be 0.189 lb. The maximum ullage temperature was 120°R. The system was simple and lightweight and, compared to an ambient helium system, would save about 150 lb, based on the experimental helium requirements.[10]

V. Conclusions

As a result of this comprehensive analytical and experimental program using a large-scale, flightweight test tank, a number of significant conclusions can be drawn regarding the applicability of a fluorine-hydrogen MTI pressurization system to a large-scale, hydrogen-fueled flight vehicle:

1) A sophisticated analytical technique has been developed that incorporates models for heat transfer, injection jet penetration, and ullage mixing, and that accurately predicts the performance of large-scale MTI pressurization systems. The analytical method accurately predicted the GF_2 usage, the tank temperature distributions, and the quantities of LH_2 evaporated over a wide range of operating conditions and injector configurations.

2) The experimental program successfully demonstrated the operation of a complete MTI pressurization control system in a large-scale, flightweight LH_2 tank. The tests indicated controllable pressurization, reasonable ullage-gas and tank-wall temperatures, and efficient GF_2 usage. The straight-pipe injectors provided more efficient (cooler) pressurization than the diffuser injector, as predicted by the analysis.

3) The MTI reaction product, HF, had been of concern with large-scale MTI application. The tankage and major structural components were unaffected by the HF. Some of the instrumentation inside the tank, when unprotected, was attacked by HF (together with severe heating/cooling temperature cycles). This could be avoided with suitable design. Sampling for HF in the LH_2 expelled from the tank was inconclusive, but the results implied that there was very little HF in the effluent LH_2 (less than 1 part per thousand).

4) Fluorine-hydrogen MTI pressurization has been tested and evaluated extensively so that flight-vehicle application can be confidently undertaken. Analysis of a typical advanced upper-stage vehicle with a multiple-burn mission, performed with the MTI pressurization computer program, indicated superior performance and substantial weight savings compared to conventional helium prepressurization.

VI. References

[1] Cady, E. C., "An Investigation of Fluorine-Hydrogen Main Tank Injection Pressurization," CR-72408, (DAC-62233), April 1968, NASA.

[2] Roudebush, W. H., "An Analysis of the Problem of Tank Pressurization During Outflow," TN D-2585, Jan. 1965, NASA.

[3] "Fortran Program for the Analysis of a Single-Propellant Tank Pressurization System," Rept. S&ID IDWA 5835, June 15, 1964, Rocketdyne Corp., Canoga Park, Calif.

[4] Kendle, D. W., "A Tank Pressurization Computer Program for Research Applications," MDAC Rept. DAC-63076, Dec. 1968, McDonnell Douglas Astronautics Co., Huntington Beach, Calif.

[5] Kendle, D. W., "Ullage Mixing Effects on Cryogenic Tank Pressurization," MDAC Rept. DAC-63168, March 1968, McDonnell Douglas Astronautics Co., Huntington Beach, Calif.

[6] Laufer, J., "Turbulent Shear Flows of Variable Density," *AIAA Journal*, Vol. 7, No. 4, April 1969, p. 706–713.

[7] Cady, E. C. and Kendle, D. W., "Vehicle-Scale Investigation of a Fluorine-Hydrogen Main Tank Injection Pressurization System," CR-72756, (MDC G0805), July 1970, NASA.

[8] DeWitt, R. L., Stochl, R. J., and Johnson, W. R., "Experimental Evaluation of Pressurant Gas Injectors During the Pressurized Discharge of Liquid Hydrogen," TN D-3458, June 1966, NASA.

[9] McAdams, W. H., *Heat Transmission*, McGraw-Hill, New York, 1954.

[10] Lacovic, R., "A Comparison of Experimental and Calculated Helium Requirements for the Pressurization of a Centaur Liquid Hydrogen Tank," TM X-1870, Sept. 1969, NASA.